Interleukin-13 reduces bone erosion in rheumatoid arthritis by up-regulating osteoprotegerin expression in fibroblast-like synoviocytes: an *in vitro* and *in vivo* study

Z. Chen[1], Z. Cheng[1], Z. Tang[2], M. Li[1], X. Tang[1], H. Zhang[1], L. Sun[1]

[1]Department of Rheumatology and Immunology, Nanjing Drum Tower Hospital, The Affiliated Hospital of Nanjing University Medical School, Nanjing, China; [2]Department of Rheumatology and Immunology, Nanjing Drum Tower Hospital, Clinical College of Nanjing Medical University, Nanjing, China.

Abstract

Objective

Bone erosion in rheumatoid arthritis (RA) is partly caused by excessive activation of osteoclasts. Osteoclasts can be derived from RA synovium and their differentiation can be inhibited by osteoprotegerin (OPG), a decoy receptor of the osteoclastogenesis-promoting cytokine receptor activator of nuclear factor κB ligand (RANKL). Fibroblast-like synoviocytes (FLSs) are the main stromal cells in the synovium that can secret OPG. The OPG secretion of FLSs can be modulated by various cytokines. Interleukin (IL)-13 can alleviate bone erosion in RA mouse models, but the mechanisms remain unclear. Therefore, we aimed to investigate whether IL-13 can induce OPG secretion by RA-FLSs, thus ameliorating bone destruction in RA by inhibiting osteoclast differentiation.

Methods

OPG, RANKL, and IL-13 receptors expression by RA-FLSs were evaluated by RT-qPCR. OPG secretion was determined by ELISA. Western blot was performed to analyse OPG expression and the activation of the STAT6 pathway. IL-13 and (or) OPG siRNA pre-treated RA-FLSs conditioned medium were used in osteoclast induction to test if IL-13 can inhibit osteoclastogenesis by up-regulating OPG in RA-FLSs. Micro-CT and immunofluorescence were performed to determine if IL-13 can induce OPG expression and alleviate bone erosion in vivo.

Results

IL-13 can promote OPG expression of RA-FLSs, and the promotion can be overcome by IL-13Rα1 or IL-13Rα2 siRNA transfection, or STAT6 inhibitor. Osteoclast differentiation can be inhibited by IL-13 pre-treated RA-FLSs conditioned medium. The inhibition can be reversed by OPG siRNA transfection. IL-13 injection can increase OPG expression in the joints while reducing bone destruction in collagen-induced arthritis mice.

Conclusion

IL-13 can inhibit osteoclastogenesis by up-regulating OPG in RA-FLSs through IL-13 receptors via the STAT6 pathway, thus may ameliorate bone erosion in RA.

Key words

rheumatoid arthritis, synoviocytes, interleukin-13, osteoclasts

*Ziyan Chen, MS**
*Zixue Cheng**
*Zhicheng Tang**
Mei Li
Xiaojun Tang, PhD
Huayong Zhang, MD, PhD
Lingyun Sun, MD, PhD

**These authors contributed equally.*

Please address correspondence to:
Huayong Zhang
Department of Rheumatology and Immunology,
Nanjing Drum Tower Hospital,
The Affiliated Hospital of Nanjing University Medical School,
321 Zhongshan Road,
Nanjing 210008, China.
E-mail: huayong.zhang@nju.edu.cn

and to:
Xiaojun Tang
(address as above)
E-mail: xjtang09@163.com

Received on November 5, 2022; accepted in revised form on February 27, 2023.

Funding: the study is supported by the National Natural Science Foundation of China (grant number 81671608, 81971525) and the Key Project supported by the Medical Science and Technology Development Foundation, Nanjing Department of Health (ZKX19020).

Competing interests: none declared.

Introduction

Rheumatoid arthritis (RA) is an autoimmune disease characterised by synovium hyperplasia, synovitis, and bone erosion, leading to irreversible joint damage and disability (1). Bone destruction is caused by excessive osteoclast activity that breaks the balance with osteoblasts (2).

Osteoprotegerin (OPG) functions as a decoy receptor for receptor activator of nuclear factor κB ligand (RANKL), which prevents RANKL binding to RANK, thus inhibiting osteoclast activation and differentiation. The RANKL-RANK-OPG system is critical in bone metabolism. By regulating RANKL to OPG ratio, osteoclast function can be kept under control (3).

In RA, osteoclast activity becomes dysregulated (4, 5). A previous study reported that osteoclast precursors and mature osteoclasts are present in the RA synovium (6). Meanwhile, OPG and RANKL are both detected in the synovium of active RA, and the RANKL to OPG ratio in synovial tissue correlates positively with the bone resorption capacity of osteoclasts derived from the same samples (7).

Fibroblast-like synoviocytes (FLSs) are the main stromal cells in the synovium and can spontaneously secret a high level of OPG (8). FLSs of RA patients (RA-FLSs) secret significantly less OPG than FLS of osteoarthritis patients (9). In the inflamed synovium of active RA, they also become a major source of RANKL, supporting osteoclast differentiation and function (10-12). As FLSs and osteoclast precursors are located adjacent to each other in RA synovium(11, 13), the secretion of OPG by FLSs may play an important role in regulating mature osteoclasts that cause bone erosion.

Various cytokines can regulate OPG expression by FLSs. For example, IL-4, IL-35, and TNF-α all can promote OPG secretion. While IL-4 and IL-35 also decrease RANKL, thus ameliorating RA bone destruction, TNF-α simultaneously increases RANKL, up-regulating RANKL to OPG ratio, thus favouring osteoclastogenesis (14, 15).

IL-13 is a cytokine mainly secreted by activated Th2 cells and shares many similarities with IL-4 (16, 17). It is significantly elevated in the synovial fluid of early RA patients compared to osteoarthritis patients or healthy controls but decreases significantly with RA progression (18). A previous study showed that IL-13 may play a protective role against bone destruction. It can reduce bone resorption in mouse calvariae and inhibit osteoclastogenesis by mouse spleen cells and bone marrow macrophages (19). Meanwhile, it decreases RANKL to OPG ratio in mouse osteoblasts (20). In RA, IL-13 is recognised as a potential anti-arthritic cytokine whose early increase in the synovial fluid was observed as a self-modulatory response (16, 21). The modulatory effect of IL-13 in RA is of interest. It has been reported that IL-13 gene therapy can ameliorate radiological score in adjuvant-induced arthritis rats, however, the underlying mechanisms were not further investigated (22).

IL-13 inhibits FLSs proliferation, reduces pro-inflammatory cytokine production of RA-FLSs, and protects FLSs from apoptosis (23, 24). We assume that, like IL-4, IL-13 can alter RANKL and OPG expression by FLSs in RA. Moreover, given the abundance of IL-13 in RA synovial fluid, as well as the excessively proliferated FLSs that IL-13 can modulate, this alteration may contribute to osteoclast regulation in RA synovium.

This study investigated whether IL-13 can induce OPG secretion by RA-FLSs, thus ameliorating bone destruction in RA by inhibiting osteoclast differentiation.

Materials and methods

Animals

Eight-week male DBA/1 mice were purchased from Chares River (China). Mice were housed in a SPF environment. All the procedures were approved by the Institutional Animal Care and Use Committee of the Affiliated Drum Tower Hospital of Nanjing University Medical School (no. 2020AE01061).

Collagen-induced arthritis (CIA) mouse model induction and treatment

CIA was induced as previously described (25). Briefly, Bovine type II

collagen (Chondrex, USA) was dissolved at 4°C overnight in acetic acid and emulsified with an equal volume of complete or incomplete Freund's adjuvant (Chondrex, USA). Mice were immunised with 100 μg of type II collagen by intradermal injection at the base of the tail on day 1 or day 21. Arthritis scoring was performed from day 28 onwards every other day according to the previous protocol (25). 15 days after the first immunisation, CIA mice were injected intravenously with 1μg IL-13 (Genescript, China) or Phosphate buffered saline (PBS) 5 times every other day. DBA/1 mice served as the control. All mice were sacrificed on day 58.

Patients

Seven RA patients who underwent joint replacement surgery were given informed consent for synovial tissue collection. These patients fulfilled either the 2010 American College of Rheumatology (ACR)/The American College of Rheumatology/European League Against Rheumatism (now European Alliance of Associations for Rheumatology, EULAR) classification criteria or the 1987 ACR classification criteria (26, 27). Synovial tissues were obtained during the surgery and were numbered RASF1 to RASF7, respectively. The baseline clinical characteristics of the included patients were shown in Supplementary Table S1. Blood samples used for osteoclastogenesis were from healthy volunteers with informed consent. This study was approved by the Ethics Committee of the Affiliated Drum Tower Hospital of Nanjing University Medical School (no. 2021-544-01).

Isolation, identification, and culture of FLSs

After rinsing three times in PBS, tissues were minced into small pieces and digested in 0.2% of type I collagen (Sigma, USA) dissolved in Dulbecco's modification of Eagle's medium-F12 (DMEM-F12) for 10 hours at 37°C in 5% CO_2. Subsequently, the digestion was terminated by DMEM-F12 with 15% FBS. Then, the cells suspension underwent a 100 μm cell strainer (FALCON, USA), rinsed three times with PBS, and re-suspended in DMEM-F12 with 15% fetal bovine serum (FBS, ExCell Bio, China) and 1× penicillin/streptomycin (Hyclone, USA). Cells were cultured for 24h to allow adherence before the culture media were changed to remove non-adherent cells, and the FBS concentration was reduced to 10%. The culture media were changed every 2 or 3 days and the cells were passaged at 80% confluence. In passage 3, cells were identified by immunofluorescence staining and flow cytometry. For flow cytometry, cells were incubated for 20 minutes at room temperature with anti-CD11b, anti-CD14, anti-CD34, anti-CD45, anti-CD79a, anti-HLA-DR, anti-CD44, anti-CD73, anti-CD90 and anti-CD146 antibody (BioLegend, 1:200). Flow cytometry was performed on BD AriaIII flow cytometer and analysed on FlowJo_v. 10 software. Passages 3-8 were used for experiments, dur-

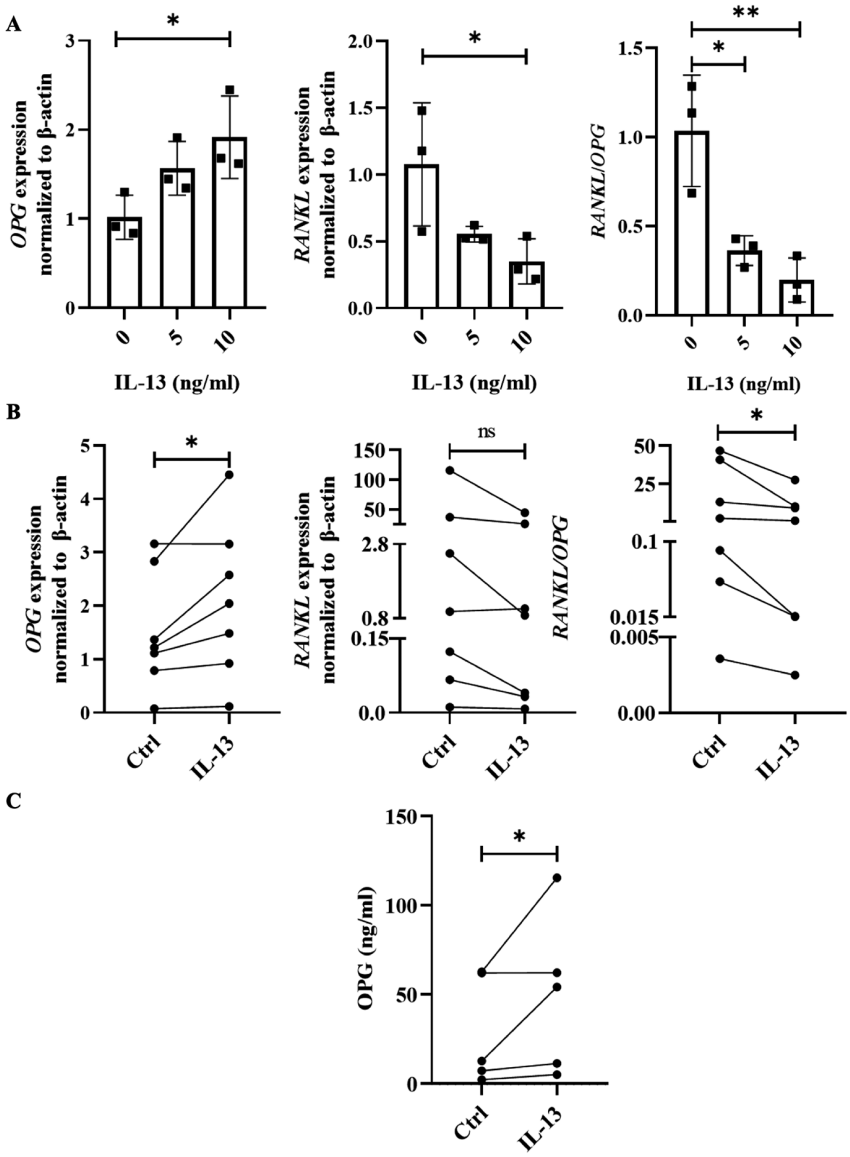

Fig. 1. IL-13 upregulates OPG and downregulates RANKL expression in RA-FLSs.
A: FLSs from 1 RA patient were stimulated by 5 ng/ml and 10 ng/ml IL-13 for 48 hours. FLSs without stimulation served as control. The OPG, RANKL mRNA levels, and RANKL/OPG ratio were analysed.
B: FLSs were stimulated by 10 ng/ml IL-13 for 48 hours. FLSs without stimulation served as control (n=7). The OPG, RANKL mRNA levels, and RANKL/OPG ratio were analysed.
C: FLSs were stimulated by 10 ng/ml IL-13 for 72 hours after the cells reached 80% confluence. OPG in the supernatants was measured by ELISA. The experiments were performed in triplicate and the mean OPG concentration for FLSs from each origin was analysed. FLSs without stimulation were used as control (n=5).

ing which more than 90% of the cells were spindle-shaped and expressed surface markers CD44, CD73, CD90, and CD146 (see Suppl. Fig. S1).

RT-qPCR

FLSs were plated in 12 well plates and stimulated by 10ng/ml IL-13 for 48 hours (Fig. 1A-B) or 24 hours (Fig. 2C). All stimulation in our experiments was performed with serum starvation overnight. FLSs without stimulation were used as control. Total RNA was extracted from FLSs with TRIzol reagent (Invitrogen, USA). cDNA was synthesised from 1μg RNA using HiScript II Q RT SuperMix II (Vazyme Biotech, China). Real-time PCR was performed using SYBR Green Master Mix (High ROX Premixed, Vazyme Biotech, China). The primers used were: hACTB: 5'-CACCATTGGCAATGAGCGGTTC-3' (forward), 5'-AGGTCTTTGCGGATGTCCACGT -3' (reverse); hOPG: 5'-GGTCTCCTGCTAACTCAGAAAGG-3' (forward), 5'-CAGCAAACCTGAAGAATGCCTCC-3' (reverse); hRANKL: 5'-ACCAGCATCAAAATCCCAAG-3' (forward), 5'-CCCCAAAGTATGTTGCATCC-3' (reverse). hIL13RA1: 5'- CGCGCCTACGGAAACTCA-3' (forward), 5'-GGGGTACTTCTATTGAACGACGA-3' (reverse) hIL13RA2: 5'-CTGGTCAGAAGTGTGCCTGT-3' (forward), 5'-AAGCATCCGATAGCCAAGCA-3' (reverse). The Step One Plus system was used to perform the real-time PCR process. The reaction procedure was set as 95°C for 5 minutes, then 95°C for 10 seconds and 60°C for 30 seconds repeating for 40 cycles, followed by 95°C for 15 seconds, 60°C for 60 seconds, and 95°C for 15 seconds. Data were processed by Step One Software, v. 2.1 (Applied Biosystems) and analysed using the $2^{-\Delta\Delta Ct}$ method, normalised to β-actin.

Enzyme-linked immunosorbent assay

RA-FLSs were stimulated by 10ng/ml IL-13 for 72 hours upon reaching 80% confluence. FLSs without stimulation served as control. Then, the supernatants were collected and centrifugated for 10 minutes at 2500×rpm, after which the supernatants were diluted accordingly from 1:10 to 1:200, and analysed by Enzyme-linked immunosorbent assay (ELISA) using Human OPG ELISA Kit (Multi Sciences, China). FLSs from each origin with or without IL-13 stimulation were measured three times. The mean OPG concentrations of the three measurements were calculated.

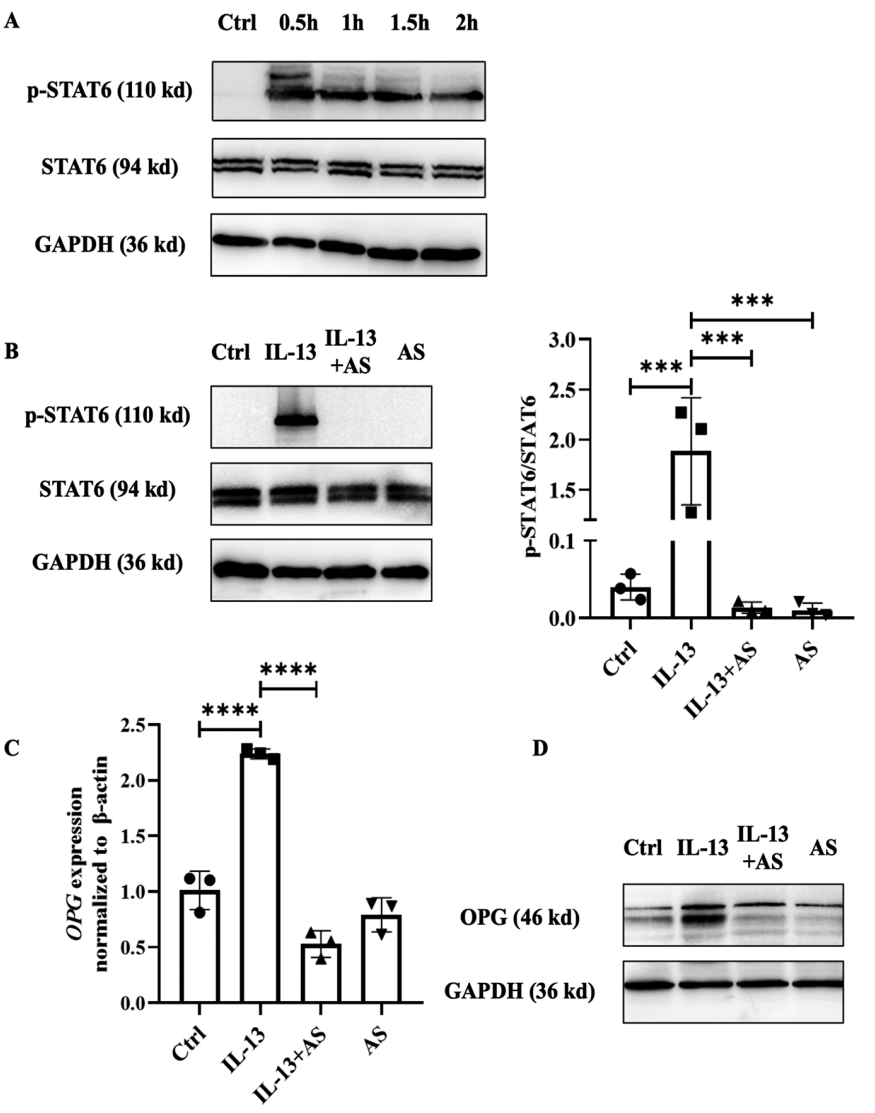

Fig. 2. IL-13 increases OPG expression of RA-FLSs via the STAT6 pathway.
A: Western Blot analysed time kinetics of STAT6 phosphorylation in RA-FLSs stimulated by 10 ng/ml IL-13.
B-D: RA-FLSs were treated with 10ng/ml IL-13 and/or 10nM STAT6 inhibitor (AS1517499) for 24 to 72 hours. STAT6 phosphorylation was analysed by Western Blot. The relative grey values (grey values of p-STAT6 /grey values of STAT6) were shown (n=3) (**B**). OPG mRNA expression was analysed by RT-qPCR (n=3) (**C**). OPG protein expression was analysed by Western Blot (**D**).

Western blotting

FLSs were plated in 6-well plates. To investigate if IL-13 can induce OPG via the STAT6 pathway, cells were stimulated by 10 ng/ml IL-13 or 10nM STAT6 inhibitor AS1517499 after reaching 80% confluence for indicated time points. In Figure 2A, FLSs were stimulated by IL-13 and (or) the STAT6 inhibitor for 0.5 to 2 hours. In Figures 2B and D, the stimulation time was 48 hours and 72 hours, respectively. FLSs without stimulation served as control. To determine which receptor was mainly responsible for IL-13-induced OPG expression, FLSs were simultaneously or sequentially treated with small interfering RNA (siRNA) of IL13 receptors and 10ng/ml IL-13 for indicated time points (Fig. 3B and D). The

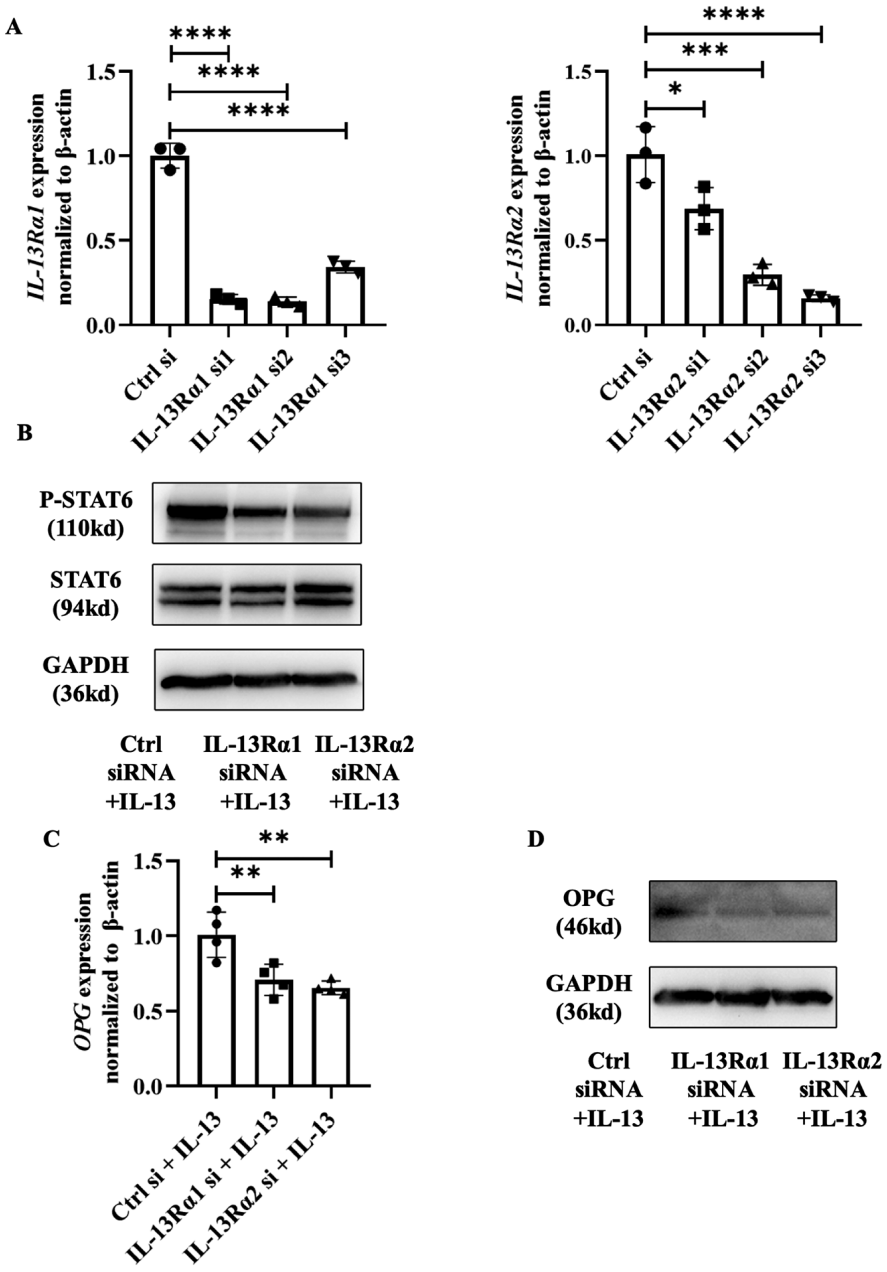

Fig. 3. IL-13 increases OPG expression of FLSs via IL-13Rα1 and IL-13Rα2.
A: IL-13Rα1 and IL-13Rα2 siRNA pre-treatment for 24 hours significantly inhibited IL-13 receptor expression in RA-FLSs (n=3).
B: For STAT6 phosphorylation measurement, FLSs were transfected by siRNAs for 72 hours, followed by 10 ng/ml IL-13 stimulation for 30 minutes.
C: For OPG mRNA expression, FLSs were pre-treated with siRNAs for 48h, after which the culture media were replaced and the FLSs were stimulated by 10 ng/ml IL-13 for 24 hours. OPG mRNA was measured by RT-qPCR (n=4).
D: For OPG protein expression, FLSs were treated with siRNAs and IL-13 for 48 hours, after which the culture media were replaced and the FLSs were stimulated by 10 ng/ml IL-13 for 24 hours. OPG protein was measured by Western Blot.

culture media were then removed and cells were rinsed twice with pre-cold PBS on ice. Subsequently, 80μl pre-cold RIPA buffer (New Cell & Molecular Biotech, China) with 1% proteinase inhibitor and 2% phosphatase inhibitor (Epizyme, China) was added to each well. After 30 minutes of incubation on ice, the cell lysates were collected and centrifuged at 12000×rpm, 4°C for 20 minutes. The protein concentration of the supernatants was measured using the Micro BCA Protein assay Kit (Thermo, USA). The supernatants were added with loading buffer (servicebio, China) and boiled subsequently. The protein samples were then separated on 10% acrylamide/bis-SDS gels (Epizyme, China) and transferred onto polyvinylidene fluoride membranes (Millipore). After blocking with 5% BSA (Sinopharm Chemical Reagent Co., Ltd., China) at room temperature for 1 hour, the membranes were incubated with primary antibodies against GAPDH (CST, USA, 1:2000), OPG (Affinity Biosciences, China, 1:1000), p-STAT6 (CST, USA, 1:1000) or STAT6 (Proteintech, China, 1:2000) at 4°C overnight. The following day the membranes were washed for 10 minutes in PBS-Tween 4 times and incubated in secondary antibodies (CST, USA 1;4000) for 1 hour at room temperature. The washing process was then repeated before the bands were scanned by the Tanon-5200 chemiluminescent imaging system. Semi-quantification was done by ImageJ Software v. 1.8.0.

Small interfering RNA transfection

FLSs were transfected with commercially available siRNAs of OPG, IL13RA1, IL13RA2, and control siRNA (Ribobio, China) using riboFECT™ CP Transfection Kit (Ribobio, China), according to the manufacturer's instructions. Cells reaching 50% confluence were incubated with 50 nm siRNA for 24 hours or 48 hours before RT-qPCR and western blot assessment, respectively.

Osteoclastogenesis and TRAP staining

Fresh anticoagulant venous blood was centrifuged at 1500×rpm for 10 minutes to remove the serum. The remaining blood cells were then diluted 1:1 by PBS. The diluted samples were then carefully layered on top of an equal volume of Ficoll (Lymphoprep™, Alere Technologies AS, Norway) and centrifuged for 20 minutes at 1500×rpm with no brake. Peripheral blood mononuclear cells (PBMCs) were then isolated and washed in PBS by centrifugation at 1500×rpm for 10 minutes. Subsequently, PBMCs were resuspended in alpha-MEM (meilunbio, China) with 10% FBS and 1% penicillin-streptomycin at 5×10^6 cells/ml and plated in 24-well

plates (1ml per well). The cells were cultured for 24 hours at 37°C, 5% CO_2 before changing the culture medium to remove non-adherent cells, and 25ng/ml human macrophage colony-stimulating factor (hM-CSF, R&D, USA) was added to the new culture medium (day 1). Three days later the culture medium was changed again (day 4). The medium of the positive control groups (Fig. 4 group a and Fig. 5 group a) were supplemented by 25 ng/ml hM-CSF and 50 ng/ml hRANKL (R&D, USA) from day 4 to day 10. To test if IL-13 can inhibit osteoclastogenesis via RA-FLSs, RA-FLSs were treated with or without 10 ng/IL-13 for 48 hours upon FLSs reaching 80% confluence. (To ensure the up-regulation of OPG on FLSs last after IL-13 withdrawal, the medium was changed after IL-13 stimulation for 48 hours, instead of 72 hours as in the ELISA experiment shown in Figure 1C). The culture media were changed and the new media were collected after another 72 hours. Then, the collected culture media passed through 0.22 μm filters and were stored at -80°C as a conditioned medium. For Figure 4 - group b, at day 4, the new culture medium contained 80% alpha-MEM with 10% FBS and 1% penicillin-streptomycin, and 20% conditioned medium pre-treated by IL-13, supplemented by 25 ng/ml hM-CSF and 50 ng/ml hRANKL. For Figure 4 group c, the new culture media were the same as group b except that the conditioned medium came from FLSs without IL-13 stimulation. The culture media were changed on day 7 with the same media as day 4. To test if IL-13 pre-treated FLSs conditioned medium inhibited osteoclastogenesis through increased OPG, FLSs were treated with OPG or control siRNAs for 48 hours and/or without IL-13, after that which the culture media was changed into DMEM-F12 (10%FBS, 1% penicillin-streptomycin). Another 72 hours later, the culture media were collected and filtered as a conditioned medium. In Figure 5, group b-e, 20% conditioned medium from different-treated FLSs were added from day 4 to day 10. On day 10, osteoclastogenesis was terminated and tartrate-resistant acid phosphatase (TRAP) staining was performed with TRAP/ALP Stain Kit (WAKO, Japan). Cells that are TRAP-positive and with more than 3 nuclei were counted as osteoclasts under the microscope in 15 separate fields.

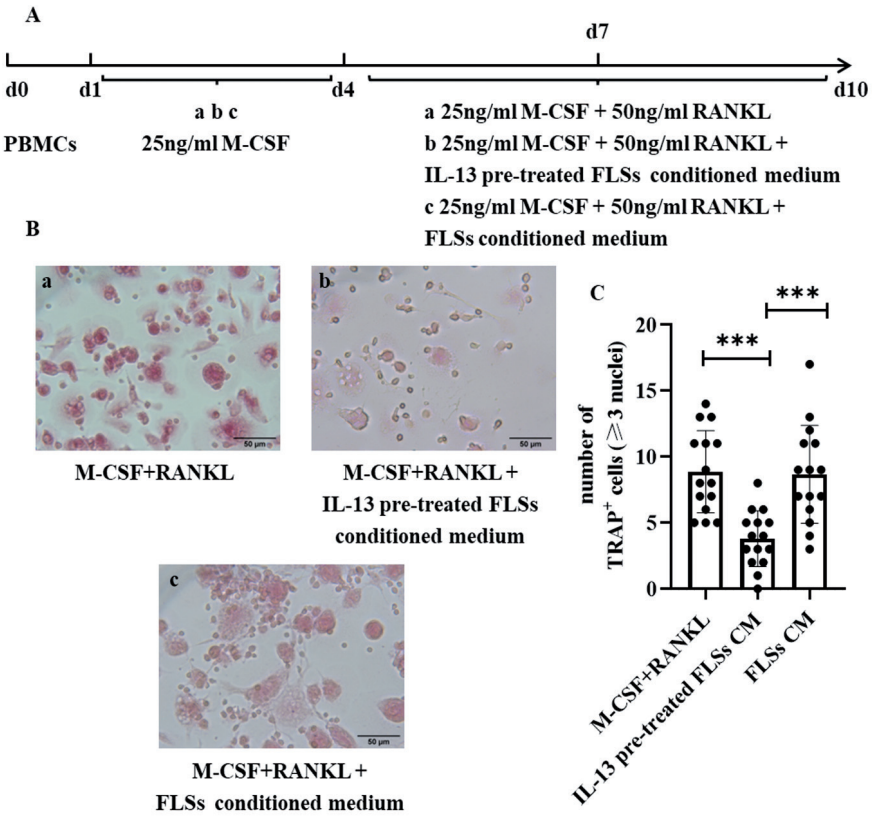

Fig. 4. IL-13 pre-treated FLSs conditioned medium inhibits osteoclast differentiation by PBMCs.
A: PBMCs were isolated and cultured for 24 hours. Adherent cells were then cultured with 25 ng/ml M-CSF for 3 days before starting osteoclast induction. Group (a) was treated with 25 ng/ml M-CSF + 50 ng/ml RANKL from day 4 to day 10. Groups (b) and (c) were cultured with conditioned medium from FLSs with or without IL-13 pre-treatment, supplemented with 25 ng/ml M-CSF + 50 ng/ml RANKL.
B: shows the representative images of the TRAP staining of each group.
C: For groups (a) (b) and (c), TRAP-positive cells with ≥3 nuclei were counted as osteoclasts in 15 separate fields. CM: conditioned medium. (Scale bars = 50 μm).

Micro-CT

After soft tissue removal and fixation, the hind paws of the mice were scanned by micro-CT (vivaCT 80, Scanco Medical, Switzerland) at 10 μm resolution. Regions of interest (ROIs) ranged from the beginning of the first cuneonavicular joint to 1mm distal to the joint. Quantitative data of trabecular bone volume/total volume (BV/TV), trabecular number (Tb.N), and trabecular separation (Tb.Sp) of plate model were acquired by Scano Evaluation software (Scanco Medical, Switzerland).

Immunofluorescence staining

Cells cultured on cell climbing slices were fixed in 4% paraformaldehyde for 30 minutes, permeabilised for 10 minutes, and blocked by 3% BSA (Sinopharm Chemical Reagent Co., Ltd., China) for 30 minutes at room temperature before incubated in anti-Vimentin (Proteintech, China, 1:200) and anti-ACTA2 (α-SMA) (Abcam, USA, 1:500) at 4°C overnight. After rinsing in PBS 3 times, the secondary antibody (Jackson ImmunoResearch Inc., USA, 1:200) was added. The sections were incubated at 37°C for 50 minutes in the dark before counterstaining with 4',6-diamidino-2-phenylindole (DAPI, Solarbio, China) for 10 minutes at room temperature in the dark. The slices were slightly dried and sealed with anti-fluorescence quenching tablets.

The paraffin-embedded mice ankle joints were cut into 5-μm sections and dewaxed to water. Then, the sections were soaked in citrate buffer (pH 6.0

Wuhan Pinuofei Biological Technology Co., Ltd, China) and boiled for 10 minutes for antigen retrieval. After rinsing in PBS for 5 minutes each time 3 times, the sections were blocked by goat serum at 37°C for 30 minutes and incubated with anti-OPG (Affinity, China, 1:100) and anti-Vimentin (Proteintech, China, 1:100) at 4°C overnight. After washing for 5 minutes 3 times in PBS, the secondary antibodies (Jackson ImmunoResearch Inc., USA) were added. The sections were incubated at 37°C for 50 minutes in the dark before counterstaining with DAPI for 10 minutes at room temperature in the dark. The sections were slightly dried and sealed with anti-fluorescence quenching tablets. The images were observed using a confocal microscope (Nikon, Japan).

Statistical analysis

Graphpad Prism 8.0 software was used for statistical analysis. Data were expressed as mean ± standard deviation (SD). Paired data from two groups with non-normal distribution were analysed by the non-parametric Wilcoxon signed-rank test. Multiple group comparisons of normally distributed data were conducted using an analysis of variance (ANOVA). Paired data from multiple groups with non-normal distribution were compared by the Friedman test. $p<0.05$ was considered statistically significant. p-values: ns, $p\geq0.05$; *$p<0.05$; **$p<0.01$; ***$p<0.001$; ****$p<0.0001$.

Results

IL-13 upregulates OPG and downregulates RANKL expression in RA-FLSs

To evaluate if IL-13 can promote OPG expression in RA-FLSs, FLSs from 1 RA patient were stimulated by 5 ng/ml or 10 ng/ml IL-13 for 48 hours. FLSs without stimulation were used as control. OPG expression increased significantly upon stimulation by 10 ng/ml IL-13. Meanwhile, RANKL expression of the FLSs significantly decreased. As it has been found that the RANKL/OPG ratio controls osteoclast differentiation, the RANKL/OPG ratio with and without IL-13 stimulation was calculated. The RANKL/OPG ratio was also significantly downregulated by 5 ng/ml or 10 ng/ml IL-13 (Fig. 1A). To determine if IL-13 can induce OPG expression in RA-FLSs in general, FLSs from 7 RA patients were stimulated by 10 ng/ml IL-13. RT-qPCR shows that IL-13 can significantly increase OPG expression and decrease RANKL/OPG ratio (Fig. 1B). ELISA was performed to confirm that IL-13 can induce OPG protein secretion of FLSs. 10 ng/ml IL-13 stimulation for 72 hours can significantly promote OPG secretion. (Fig. 1C).

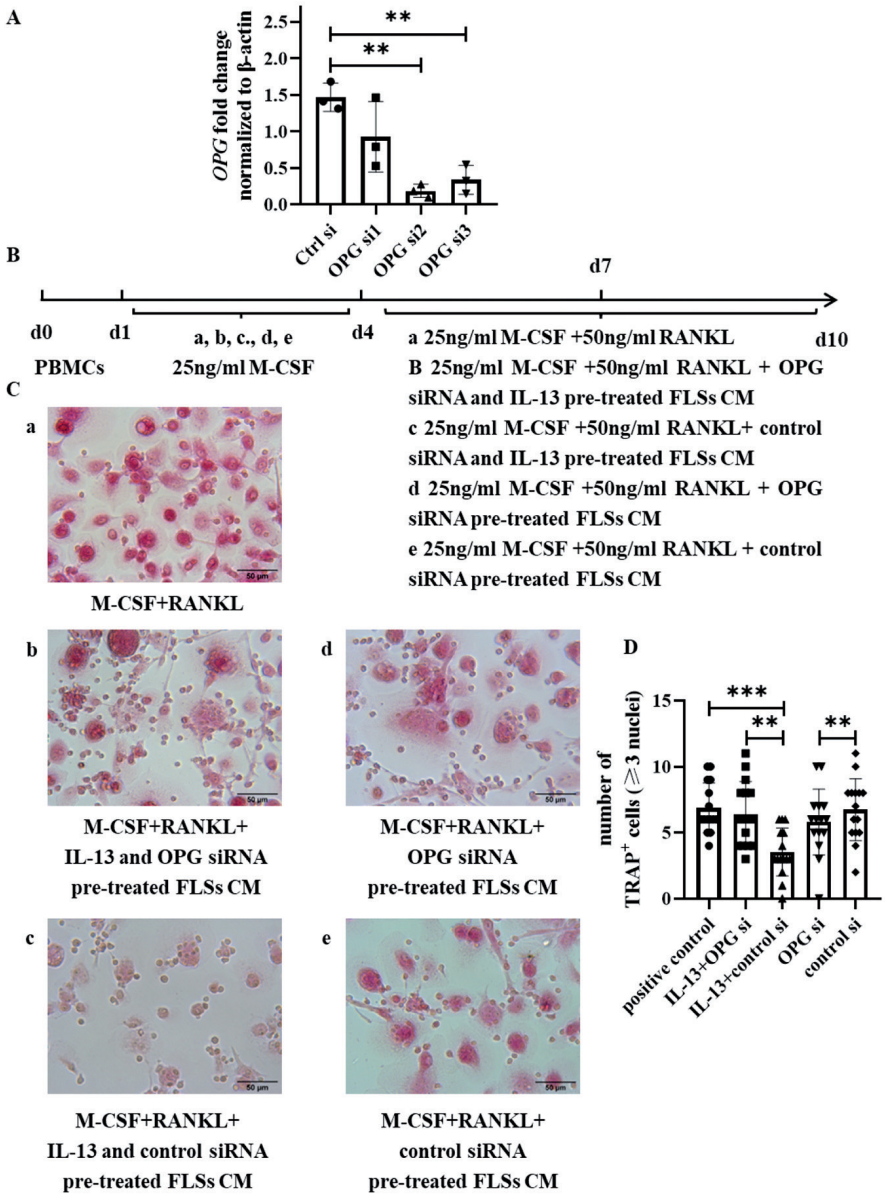

Fig. 5. IL-13 pre-treated FLSs inhibit osteoclast differentiation by increased OPG.
A: FLSs were treated with control siRNA (ctrl si) and 3 OPG siRNAs (OPG si1 to OPG si3) for 24 hours. OPG mRNA expression was measured by RT-qPCR (n=3).
B: Osteoclast induction was carried out as indicated. Group (**a**) was treated with 25 ng/ml M-CSF + 50 ng/ml RANKL from day 4 to day 10. Groups (**b**), (**c**), (**d**), and (**e**) were cultured with FLSs conditioned medium supplemented with 25 ng/ml M-CSF + 50 ng/ml RANKL. The FLSs conditioned medium of groups (**b**), (**c**), (**d**), and (**e**) were prepared as described in materials and methods. CM: conditioned medium.
C: Shows the representative images of TRAP staining of each group.
D: TRAP-positive cells with ≥3 nuclei were counted as osteoclasts in 15 separate fields for Figure 5C groups (**a**) to (**e**), respectively (Scale bars = 50 μm).

IL-13 increases OPG expression of RA-FLSs via the STAT6 pathway

IL-13 is known to be able to activate the STAT6 pathway(28). To determine if IL-13 upregulates OPG via STAT6 phosphorylation, RA-FLSs were stim-

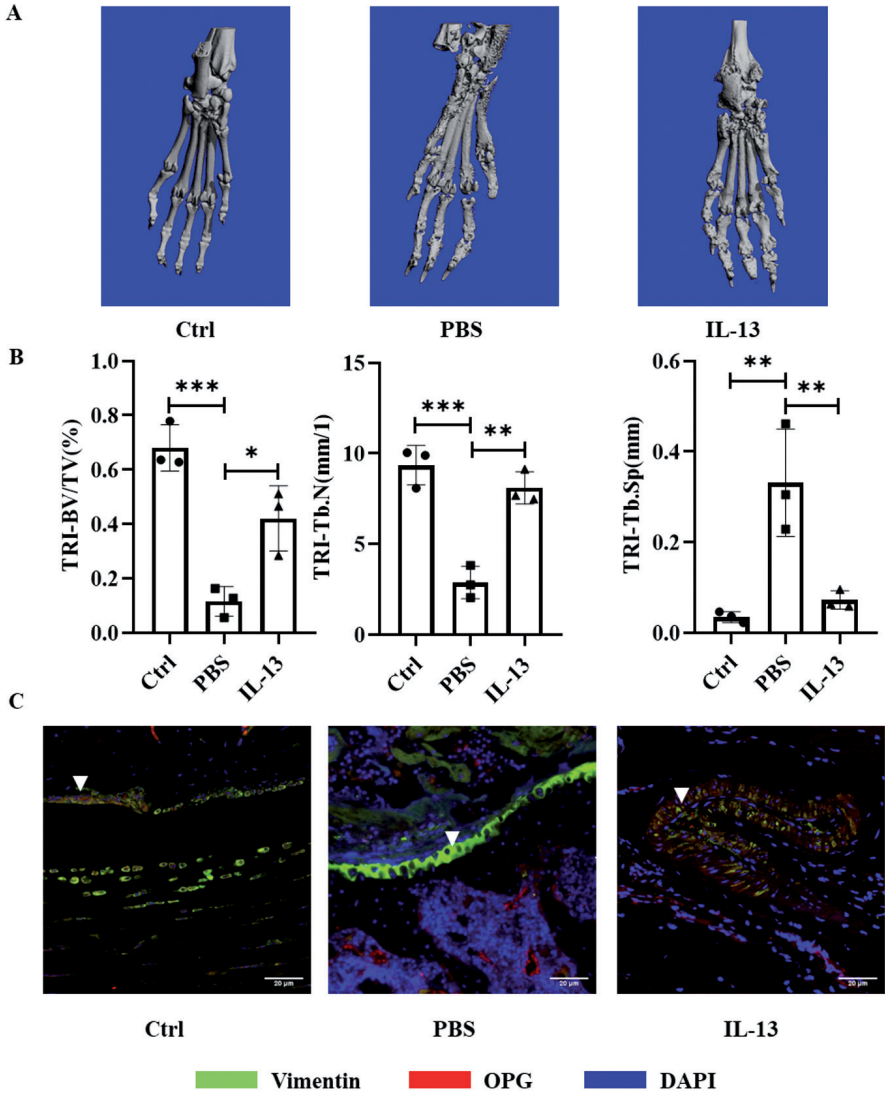

Fig. 6. IL-13 ameliorates bone erosion in CIA mice.
A: Shows the representative micro-CT images.
B: Shows the trabecular bone volume/total volume (BV/TV), and trabecular number (Tb.N) were significantly increased. Meanwhile, trabecular separation (Tb.Sp) was significantly decreased in mice treated with IL-13 than in mice injected with PBS. (n=3 in each group).
C: Immunofluorescence staining was carried out for the ankle joints of the mice from each group. The FLSs marker Vimentin and OPG were labelled with FITC and APC (Scale bars = 20 μm).

ulated by 10 ng/ml IL-13 for various time points. STAT6 phosphorylation can be detected with 30 minutes of stimulation by IL-13. (Fig. 2A). Further investigation showed that STAT6 remained phosphorylated after 48h of stimulation and can be inhibited by a STAT6 inhibitor (AS1517499, AS). The activation and inhibition of the STAT6 pathway by IL-13 and the STAT6 inhibitor were significant. (Fig. 2B). OPG mRNA and protein expression after IL-13 and STAT6 inhibitor treatment were then analysed by RT-qPCR and Western Blot, respectively. OPG mRNA expression increased after 10 ng/ml IL-13 stimulation for 24 hours and was inhibited by the inhibitor (Fig. 2C). Consistently, OPG protein level followed the same trend after IL-13 and STAT6 inhibitor treatment for 72h (Fig. 2D).

IL-13 increases OPG expression of FLSs via IL-13 receptor α1 and α2

IL-13 has two cognate receptor subunits, IL-13 Rα1 and IL-13Rα2, which specifically bind to IL-13(28). However, the precise roles of IL-13 Rα1 and IL-13Rα2 in IL-13 signalling and response are not clear. To further explore which receptor did IL-13 induce OPG in RA-FLSs, FLSs were transfected with siRNAs of IL-13Rα1 or IL-13Rα2. RT-qPCR was performed to validate the silencing efficiency after 24h. (Fig. 3A). The siRNAs of the highest efficiency were used to knock down each IL-13 receptor. Compared with control siRNA transfected FLSs, IL-13Rα1 and IL-13Rα2 knocked down FLSs both showed reduced STAT6 phosphorylation (Fig. 3B) as well as OPG protein expression (Fig. 3C) when stimulated with IL-13. FLSs transfected with control siRNA served as control.

IL-13 pre-treated FLSs conditioned medium inhibits osteoclast differentiation by PBMCs

To discover if the increased secretion of OPG by RA-FLSs can sufficiently inhibit osteoclast differentiation, osteoclastogenesis by PBMCs was evaluated by TRAP staining. The RA-FLSs conditioned medium pre-treated with 10 ng/ml IL-13 for 48h (Fig. 4B group b) significantly inhibited osteoclastogenesis compared with positive control stimulated with M-CSF and RANKL only. (Fig. 4B group a), while the conditioned medium of RA-FLSs without treatment (Fig. 4B group c) did not significantly suppress osteoclast differentiation compared to the positive control (Fig. 4B group a), however, the osteoclasts seemed to be larger with more nuclei.

IL-13 pre-treated FLSs inhibit osteoclast differentiation by increased OPG

To further test if it is increased OPG that induces the inhibition of osteoclasts by IL-13 pre-treated RA-FLSs, FLSs were pre-treated with OPG siRNA or control siRNA along with 10 ng/ml IL-13. The OPG siRNA with the highest silencing efficiency verified by RT-qPCR (OPG si2) was selected to knock down OPG expression (Fig. 5A). The FLSs conditioned medium pre-treated by IL-13 and OPG siRNA failed to induce significant inhibition of osteoclastogenesis compared with the positive control group. (Fig. 5C group b *vs*. group a), while the conditioned medium pre-treated by IL-13 and control siRNA significantly inhibited osteoclast differentiation (Fig. 5C group c *vs*. group a).

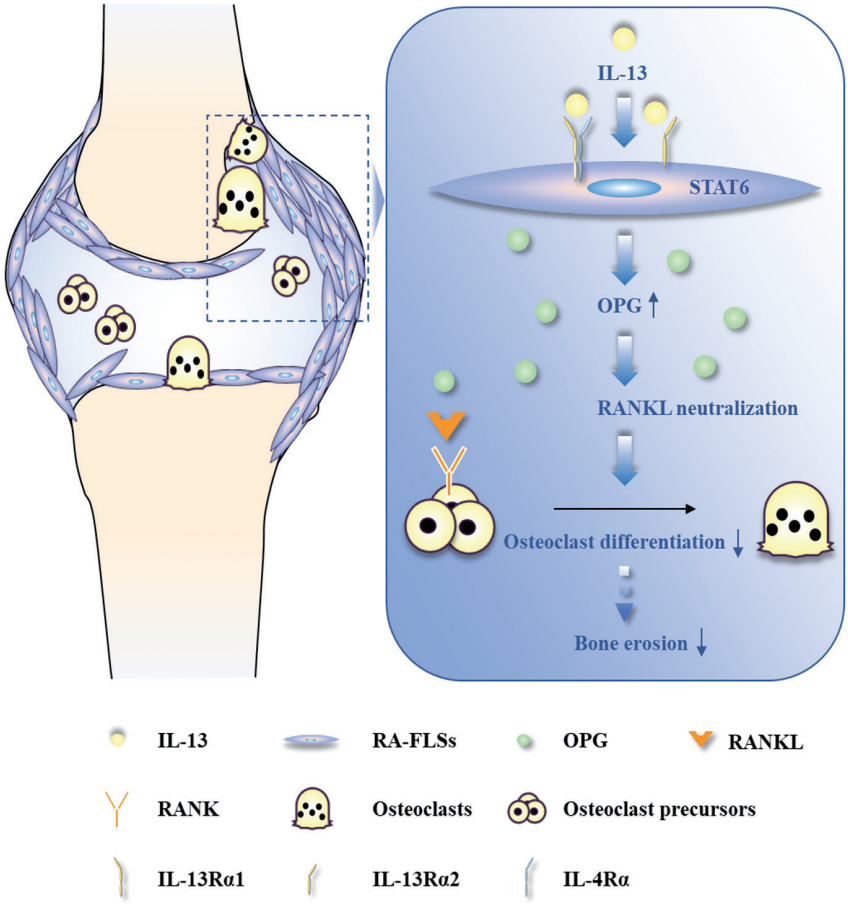

Fig. 7. Schematic of our findings.
IL-13 can inhibit osteoclastogenesis by up-regulating OPG expression of RA-FLSs via the STAT-6 pathway, thus may contribute to the amelioration of bone erosion in CIA mice *in vivo*. IL-13Rα1 and IL-13Rα2 may participate in the process.

IL-13 ameliorates bone erosion in CIA mice

Since we discovered that IL-13 may inhibit osteoclast differentiation by up-regulating OPG in RA-FLSs *in vitro*, it is interesting to know if IL-13 can also ameliorate bone erosion *in vivo* by inducing OPG expression of FLSs. Thus, micro-CT was used to test if IL-13 can reduce bone destruction in CIA mice. Figure 6A shows the representative micro-CT images of control mice and CIA mice treated with PBS and IL-13. Analysis of ROIs described in materials and methods revealed that the trabecular bone volume/total volume (BV/TV) and trabecular number (Tb.N) were significantly increased while trabecular separation (Tb.Sp) was significantly decreased in mice treated with IL-13, compared with that in mice injected with PBS (Fig. 6B). To investigate if IL-13 can up-regulate OPG in FLSs *in vivo*, Immunofluorescence staining was carried out for the ankle joint of the mice from each group. The FLSs marker Vemintin and OPG were labelled with FITC and APC. In the ankle joints of mice treated with IL-13, increased OPG colocalised with Vimentin was detected compared with the PBS group. Meanwhile, control non-arthritic mice showed thinner Vemintin -positive cells than CIA mice (Fig. 6C).

Discussion

Inflammatory bone erosion caused by imbalanced osteoclast-osteoblast activity has always been the main concern in RA. Targeting the RANKL/RANK/OPG system may suppress the abnormal activation of osteoclasts(29). It has been reported that RA-FLSs can secret OPG, and as mentioned in the introduction, the secretion can be regulated by cytokines. Other compounds, for example, oestrogen, can induce OPG expression of RA-FLSs as well (30). Our previous study also showed that the combination of sinomenine and methotrexate can up-regulate OPG mRNA expression by RA-FLS (31). However, few studies have demonstrated whether the induced OPG is sufficient for osteoclastogenesis inhibition.

In the present study, we found that FLSs from RA patients can be an abundant source of OPG. IL-13 was able to promote OPG expression of RA-FLSs through IL-13Rα1 and IL-13Rα2 via the STAT6 pathway. Meanwhile, RANKL tends to be decreased. After being pre-treated by IL-13, FLSs conditioned medium can inhibit osteoclasts differentiation *in vitro* through increased OPG. Meanwhile, intravenous administration of IL-13 alleviated bone destruction and increased OPG expression in the ankle joints of CIA mice.

When investigating OPG promotion by IL-13, we first discovered that the sensitivity to IL-13 differed among FLSs from different RA patients. The OPG fold change upon stimulation showed a positive correlation with IL-13Rα1 but no correlation with IL-13Rα2 (see Suppl. Fig. S2). However, further siRNA transfection indicated that IL-13Rα1 and IL-13Rα2 may both participate in IL-13-induced OPG expression by RA-FLSs. IL-13Rα1 and IL-13Rα2 are two subunits of the IL-13 receptors. IL-13Rα1 recruits IL-4Rα to form a complex upon binding to IL-13 with moderate affinity, activating the STAT6 pathway. IL-13Rα2 binds IL-13 with high affinity, which was initially recognised as a decoy receptor but was recently found to be capable of signal transduction. (28, 32). The correlation between IL-13Rα1 and OPG fold change implied that IL-13Rα1 and downstream STAT6 pathway might be involved in OPG induction in FLSs. Western blot analysis showed that STAT6 was phosphorylated when stimulated by IL-13. Furthermore, the OPG increase induced by IL-13 stimulation can be sufficiently blocked by a STAT6 inhibitor. After IL-13Rα1 knockdown, STAT6 phosphorylation, as well as OPG expression, both decreased. Interestingly, knocking down IL-13Rα2 can also block STAT6 phosphorylation and OPG induction by IL-13, suggest-

ing that IL-13Rα2 may also play a role in IL-13-induced OPG upregulation.

We noticed that FLSs from one RA patient, OPG secretion was doubled and reached more than 100 ng/ml in the culture media. According to the previous study (33), OPG should inhibit osteogenesis in synovial cells. Such high OPG concentration induced by IL-13 *in vitro* implied that, though IL-13 can directly inhibit osteoclast differentiation, the indirect inhibition through OPG should not be overlooked, given the crucial role OPG plays in regulating osteoclast differentiation. To eliminate the direct effect of IL-13 on FLSs, we changed the medium containing IL-13 and collected the supernatant three days later as conditioned medium to induce osteoclast differentiation. In line with our hypothesis, the conditioned medium of IL-13 pre-treated FLSs can suppress osteoclast differentiation compared with the conditioned medium without IL-13 pre-treatment and the induction system with only RANKL and M-CSF. OPG knockdown further proved that OPG was responsible for IL-13-induced osteoclastogenesis inhibition. *In vivo* experiments were consistent with *in vitro*, showing that the bone erosion of CIA mice was alleviated by IL-13 injection. We use micro-CT instead of x-ray performed by the previous study to closely observe the bone structure (22). Immunofluorescence staining also showed an increase in OPG that colocalised with Vimentin, a positive marker of mesenchymal cells in 95% of FLSs (34). However, our *in vivo* experiment did not rule out the possibility that IL-13 may attenuate bone destruction by directly inhibiting osteoclast differentiation.

FLSs have also been reported to be a main source of RANKL during inflammation (35), and since RANKL/OPG ratio is essential for osteoclast differentiation regulation (7), RANKL secretion was also measured. Surprisingly, RANKL secretion of RA-FLSs involved in this experiment was all below detection while analysed with a commercial ELISA kit, (lower detection limit 7.8 pg/ml). Flow cytometry also failed to detect membrane-bound RANKL. A previous study pointed out that FLSs in RA were heterogeneous and consisted of different subsets, among which CD90 positive ones were less likely to cause bone erosion than CD90 negative FLSs, while CD90 negative FLSs produced more RANKL (36). As the FLSs we investigated express CD90, the lack of RANKL and relatively abundant OPG secretion supports such findings. Another research also noticed that FLSs from the synovium produced far less RANKL than FLSs from the pannus tissue (10). The FLSs we investigated might have come from the synovium rather than the pannus tissue. Extra efforts should be taken to further identify the exact role played in osteoclastogenesis by different subsets of RA-FLSs.

It is also worth mentioning that the disease duration of RA patients enrolled in this study was all more than 1 year, and for 5 of 7 patients, the disease lasts for more than 10 years. Thus, our findings may better apply to long-standing RA, and studies focusing on earlier phases of the disease should be undertaken.

Nevertheless, we demonstrated for the first time that IL-13 could up-regulate OPG through IL13Rα1 and IL13Rα2 via the STAT6 pathway in RA-FLSs. Furthermore, FLSs pre-treated by IL-13 can inhibit osteoclast differentiation *in vitro* through increased OPG. As synovium hyperplasia is a hallmark of RA and large numbers of inflamed FLSs can be in contact with osteoclast precursors, inhibition of osteoclasts via up-regulating OPG in FLSs can be an important regulatory mechanism of IL-13 on bone destruction in RA (Fig. 7).

Conclusions

To sum up, we raised the possibility that some FLSs in RA can secret a relatively high level of OPG. IL-13 can up-regulate OPG in RA-FLSs through IL-13Rα1 and IL-13Rα2 via the STAT6 pathway, thus alleviating bone erosion in CIA mice by inhibiting osteoclast differentiation. These findings may provide a new perspective on the role of IL-13 in RA pathogenesis and treatment.

Acknowledgments

We thank Prof Zhihong Xu for help with synovial tissue sample collection, and all the patients and participants in this study.

References

1. AURÉAL M, MACHUCA-GAYET I, COURY F: Rheumatoid arthritis in the view of osteoimmunology. *Biomolecules* 2020; 11(1). http://doi.org/10.3390/biom11010048
2. SCHETT G, GRAVALLESE E: Bone erosion in rheumatoid arthritis: mechanisms, diagnosis and treatment. *Nat Rev Rheumatol* 2012; 8(11): 656-64. http://doi.org/10.1038/nrrheum.2012.153
3. WALSH MC, CHOI Y: Biology of the RANKL-RANK-OPG system in immunity, bone, and beyond. *Front Immunol* 2014; 5: 511. http://doi.org/10.3389/fimmu.2014.00511
4. LE GOFF B, BERTHELOT JM, MAUGARS Y, HEYMANN D: Osteoclasts in RA: diverse origins and functions. *Joint Bone Spine* 2013; 80(6): 586-91. http://doi.org/10.1016/j.jbspin.2013.04.002
5. PETRELLI F, MARIANI FM, ALUNNO A, PUXEDDU I: Pathogenesis of rheumatoid arthritis: one year in review 2022. *Clin Exp Rheumatol* 2022; 40(3): 475-82. http://doi.org/10.55563/clinexprheumatol/l9lyen
6. GRAVALLESE EM, HARADA Y, WANG JT, GORN AH, THORNHILL TS, GOLDRING SR: Identification of cell types responsible for bone resorption in rheumatoid arthritis and juvenile rheumatoid arthritis. *Am J Pathol* 1998; 152(4): 943-51.
7. HAYNES DR, CROTTI TN, LORIC M, BAIN GI, ATKINS GJ, FINDLAY DM: Osteoprotegerin and receptor activator of nuclear factor kappaB ligand (RANKL) regulate osteoclast formation by cells in the human rheumatoid arthritic joint. *Rheumatology* (Oxford) 2001; 40(6): 623-30. http://doi.org/10.1093/rheumatology/40.6.623
8. ZIOLKOWSKA M, KUROWSKA M, RADZIKOWSKA A *et al*.: High levels of osteoprotegerin and soluble receptor activator of nuclear factor kappa B ligand in serum of rheumatoid arthritis patients and their normalization after anti-tumor necrosis factor alpha treatment. *Arthritis Rheum* 2002; 46(7): 1744-53. http://doi.org/10.1002/art.10388
9. HARASHIMA SI, TSUKAMOTO H, HORIUCHI T: Osteoprotegerin and receptor activator of nuclear factor kappaB ligand expression in fibroblast-like synoviocytes from rheumatoid arthritis and osteoarthritis patients. *Rheumatology* (Oxford) 2004; 43(3): 396-97; author reply 397. http://doi.org/10.1093/rheumatology/keh022
10. AINOLA M, MANDELIN J, LILJESTRÖM M, KONTTINEN YT, SALO J: Imbalanced expression of RANKL and osteoprotegerin mRNA in pannus tissue of rheumatoid arthritis. *Clin Exp Rheumatol* 2008; 26(2): 240-46.
11. WU Y, LIU J, FENG X *et al*.: Synovial fibroblasts promote osteoclast formation by RANKL in a novel model of spontaneous erosive arthritis. *Arthritis Rheum* 2005; 52(10): 3257-68. http://doi.org/10.1002/art.21354
12. WU S, JIANG Y, TENG Y, LIU X, ZHOU L, LI W: Interleukin-33 promotes proliferation and inhibits apoptosis of fibroblast-like synoviocytes in rheumatoid arthritis. *Clin Exp Rheumatol* 2021; 39(4): 844-81. http://doi.org/10.55563/clinexprheumatol/htpmp0
13. MORI H, KITAZAWA R, MIZUKI S, NOSE M, MAEDA S, KITAZAWA S: RANK ligand,

RANK, and OPG expression in type II collagen-induced arthritis mouse. *Histochem Cell Biol* 2002; 117(3): 283-92. http://doi.org/10.1007/s00418-001-0376-9
14. TUNYOGI-CSAPO M, KIS-TOTH K, RADACS M *et al*.: Cytokine-controlled RANKL and osteoprotegerin expression by human and mouse synovial fibroblasts: fibroblast-mediated pathologic bone resorption. *Arthritis Rheum*. 2008; 58(8): 2397-408. http://doi.org/10.1002/art.23653
15. LI Y, LI D, LI Y *et al*.: Interleukin-35 upregulates OPG and inhibits RANKL in mice with collagen-induced arthritis and fibroblast-like synoviocytes. *Osteoporos Int* 2016; 27(4): 1537-46. http://doi.org/10.1007/s00198-015-3410-9
16. MAO YM, ZHAO CN, LENG J *et al*.: Interleukin-13: a promising therapeutic target for autoimmune disease. *Cytokine Growth Factor Rev* 2019; 45: 9-23. http://doi.org/10.1016/j.cytogfr.2018.12.001
17. ISOMÄKI P, LUUKKAINEN R, TOIVANEN P, PUNNONEN J: The presence of interleukin-13 in rheumatoid synovium and its antiinflammatory effects on synovial fluid macrophages from patients with rheumatoid arthritis. *Arthritis Rheum*. 1996; 39(10): 1693-702. http://doi.org/10.1002/art.1780391012
18. RAZA K, FALCIANI F, CURNOW SJ *et al*.: Early rheumatoid arthritis is characterized by a distinct and transient synovial fluid cytokine profile of T cell and stromal cell origin. *Arthritis Res Ther* 2005; 7(4): R784-795. http://doi.org/10.1186/ar1733
19. PALMQVIST P, LUNDBERG P, PERSSON E *et al*.: Inhibition of hormone and cytokine-stimulated osteoclastogenesis and bone resorption by interleukin-4 and interleukin-13 is associated with increased osteoprotegerin and decreased RANKL and RANK in a STAT6-dependent pathway. *J Biol Chem* 2006; 281(5): 2414-29. http://doi.org/10.1074/jbc.M510160200
20. YAMADA A, TAKAMI M, KAWAWA T *et al*.: Interleukin-4 inhibition of osteoclast differentiation is stronger than that of interleukin-13 and they are equivalent for induction of osteoprotegerin production from osteoblasts. *Immunology* 2007; 120(4): 573-79. http://doi.org/10.1111/j.1365-2567.2006.02538.x
21. CHEN Z, BOZEC A, RAMMING A, SCHETT G: Anti-inflammatory and immune-regulatory cytokines in rheumatoid arthritis. *Nat Rev Rheumatol* 2019; 15(1): 9-17. http://doi.org/10.1038/s41584-018-0109-2
22. WOODS JM, AMIN MA, KATSCHKE KJ JR. *et al*.: Interleukin-13 gene therapy reduces inflammation, vascularization, and bony destruction in rat adjuvant-induced arthritis. *Hum Gene Ther* 2002; 13(3): 381-93. http://doi.org/10.1089/10430340252792512
23. RELIC B, GUICHEUX J, MEZIN F *et al*.: Il-4 and IL-13, but not IL-10, protect human synoviocytes from apoptosis. *J Immunol* 2001; 166(4): 2775-82. http://doi.org/10.4049/jimmunol.166.4.2775
24. MORITA Y, YAMAMURA M, KAWASHIMA M *et al*.: Differential in vitro effects of IL-4, IL-10, and IL-13 on proinflammatory cytokine production and fibroblast proliferation in rheumatoid synovium. *Rheumatol Int* 2001; 20(2): 49-54. http://doi.org/10.1007/s002960000074
25. LIU C, ZHANG H, TANG X *et al*.: Mesenchymal stem cells promote the osteogenesis in collagen-induced arthritic mice through the inhibition of TNF-α. *Stem Cells Int* 2018; 2018: 4069032. http://doi.org/10.1155/2018/4069032
26. ALETAHA D, NEOGI T, SILMAN AJ *et al*.: 2010 Rheumatoid arthritis classification criteria: an American College of Rheumatology/European League Against Rheumatism collaborative initiative. *Arthritis Rheum* 2010; 62(9): 2569-81. http://doi.org/10.1002/art.27584
27. ARNETT FC, EDWORTHY SM, BLOCH DA *et al*.: The American Rheumatism Association 1987 revised criteria for the classification of rheumatoid arthritis. *Arthritis Rheum* 1988; 31(3): 315-24. http://doi.org/10.1002/art.1780310302
28. JUNTTILA IS: Tuning the cytokine responses: an update on interleukin (IL)-4 and IL-13 receptor complexes. *Front Immunol* 2018; 9: 888. http://doi.org/10.3389/fimmu.2018.00888
29. GEUSENS P: The role of RANK ligand/osteoprotegerin in rheumatoid arthritis. *Ther Adv Musculoskelet Dis* 2012; 4(4): 225-33. http://doi.org/10.1177/1759720x12438080
30. MITANI M, MIURA Y, SAURA R *et al*.: Estrogen specifically stimulates expression and production of osteoprotegerin from rheumatoid synovial fibroblasts. *Int J Mol Med* 2005; 15(5): 827-32.
31. SUN Y, YAO Y, DING CZ: A combination of sinomenine and methotrexate reduces joint damage of collagen induced arthritis in rats by modulating osteoclast-related cytokines. *Int Immunopharmacol* 2014; 18(1): 135-41. http://doi.org/10.1016/j.intimp.2013.11.014
32. FICHTNER-FEIGL S, STROBER W, KAWAKAMI K, PURI RK, KITANI A: IL-13 signaling through the IL-13alpha2 receptor is involved in induction of TGF-beta1 production and fibrosis. *Nat Med* 2006; 12(1): 99-106. http://doi.org/10.1038/nm1332
33. TAKAYANAGI H, IIZUKA H, JUJI T *et al*.: Involvement of receptor activator of nuclear factor kappaB ligand/osteoclast differentiation factor in osteoclastogenesis from synoviocytes in rheumatoid arthritis. *Arthritis Rheum* 2000; 43(2): 259-69. http://doi.org/10.1002/1529-0131(200002)43:2<259::Aid-anr4>3.0.Co;2-w.
34. ZHAO J, OUYANG Q, HU Z *et al*.: A protocol for the culture and isolation of murine synovial fibroblasts. *Biomed Rep* 2016; 5(2): 171-75. http://doi.org/10.3892/br.2016.708
35. DANKS L, KOMATSU N, GUERRINI MM *et al*.: RANKL expressed on synovial fibroblasts is primarily responsible for bone erosions during joint inflammation. *Ann Rheum Dis* 2016; 75(6): 1187-95. http://doi.org/10.1136/annrheumdis-2014-207137
36. CROFT AP, CAMPOS J, JANSEN K *et al*.: Distinct fibroblast subsets drive inflammation and damage in arthritis. *Nature* 2019; 570(7760): 246-51. http://doi.org/10.1038/s41586-019-1263-7.